

# Synthesis and Evaluation of $^{18}\text{F}$ -Enzalutamide, a New Radioligand for PET Imaging of Androgen Receptors: A Comparison with $16\beta$ - $^{18}\text{F}$ -Fluoro- $5\alpha$ -Dihydrotestosterone

Inês F. Antunes\*<sup>1</sup>, Rutger J. Dost\*<sup>2</sup>, Hilde D. Hoving<sup>2</sup>, Aren van Waarde<sup>1</sup>, Rudi A.J.O Dierckx<sup>1</sup>, Douwe F. Samplonius<sup>3</sup>, Wijnand Helfrich<sup>3</sup>, Philip H. Elsinga<sup>1</sup>, Erik F.J. de Vries<sup>1</sup>, and Igle J. de Jong<sup>2</sup>

<sup>1</sup>Department of Nuclear Medicine and Molecular Imaging, University Medical Center Groningen, University of Groningen, Groningen, The Netherlands; <sup>2</sup>Department of Urology, University Medical Centre Groningen, University of Groningen, Groningen, The Netherlands; and <sup>3</sup>Surgical Research Laboratory, University Medical Centre Groningen, University of Groningen, Groningen, The Netherlands

J Nucl Med 2021; 62:1140–1145

DOI: 10.2967/jnumed.120.253641

$16\beta$ - $^{18}\text{F}$ -fluoro- $5\alpha$ -dihydrotestosterone ( $^{18}\text{F}$ -FDHT) is a radiopharmaceutical that has been investigated as a diagnostic agent for the assessment of androgen receptor (AR) density in prostate cancer using PET. However,  $^{18}\text{F}$ -FDHT is rapidly metabolized in humans and excreted via the kidneys into the urine, potentially compromising the detection of tumor lesions close to the prostate. Enzalutamide is an AR signaling inhibitor currently used in different stages of prostate cancer. Enzalutamide and its primary metabolite *N*-desmethylenzalutamide have an AR affinity comparable to that of FDHT but are excreted mainly via the hepatic route. Radiolabeled enzalutamide could thus be a suitable candidate PET tracer for AR imaging. Here, we describe the radiolabeling of enzalutamide with  $^{18}\text{F}$ . Moreover, the in vitro and in vivo behavior of  $^{18}\text{F}$ -enzalutamide was evaluated and compared with the current standard,  $^{18}\text{F}$ -FDHT. **Methods:**  $^{18}\text{F}$ -enzalutamide was obtained by fluorination of the nitro precursor. In vitro cellular uptake studies with  $^{18}\text{F}$ -enzalutamide and  $^{18}\text{F}$ -FDHT were performed in LNCaP (AR-positive) and HEK293 (AR-negative) cells. Competition assays with both tracers were conducted on the LNCaP (AR-positive) cell line. In vivo PET imaging, ex vivo biodistribution, and metabolite studies with  $^{18}\text{F}$ -enzalutamide and  $^{18}\text{F}$ -FDHT were conducted on athymic nude male mice bearing an LNCaP xenograft in the shoulder. **Results:**  $^{18}\text{F}$ -enzalutamide was obtained in  $1.4\% \pm 0.9\%$  radiochemical yield with an apparent molar activity of  $6.2 \pm 10.3$  GBq/ $\mu\text{mol}$ .  $^{18}\text{F}$ -FDHT was obtained in  $1.5\% \pm 0.8\%$  yield with a molar activity of more than 25 GBq/ $\mu\text{mol}$ . Coincubation with an excess of  $5\alpha$ -dihydrotestosterone or enzalutamide significantly reduced the cellular uptake of  $^{18}\text{F}$ -enzalutamide and  $^{18}\text{F}$ -FDHT to about 50% in AR-positive LNCaP cells but not in AR-negative HEK293 cells. PET and biodistribution studies on male mice bearing a LNCaP xenograft showed about 3 times higher tumor uptake for  $^{18}\text{F}$ -enzalutamide than for  $^{18}\text{F}$ -FDHT. Sixty minutes after tracer injection, 93% of  $^{18}\text{F}$ -enzalutamide in plasma was still intact, compared with only 3% of  $^{18}\text{F}$ -FDHT. **Conclusion:** Despite its lower apparent molar activity,  $^{18}\text{F}$ -enzalutamide shows higher tumor uptake and better metabolic stability than  $^{18}\text{F}$ -FDHT and thus seems to have more favorable properties for imaging of AR with PET. However, further evaluation in other oncologic animal models and patients is warranted to confirm these results.

**Key words:** prostate cancer; PET imaging; androgen receptors; enzalutamide; mice

Received Aug. 13, 2020; revision accepted Nov. 14, 2020.

For correspondence or reprints, contact Inês F. Antunes (i.farinha.antunes@umcg.nl).

\*Contributed equally to this work.

Published online January 30, 2021.

COPYRIGHT © 2021 by the Society of Nuclear Medicine and Molecular Imaging.

**P**rostate cancer has an incidence of 1.4 million cases per year, making it the leading cause of cancer for men (1). Prostate cancer is a hormone-sensitive cancer that usually expresses androgen receptors (ARs), which play a prominent role in the development and treatment of the disease (2). The cornerstone of treatment has been androgen deprivation therapy or, if unsuccessful, chemotherapy (2,3). In more recent years, other hormonal therapies that focus on inhibition of AR-mediated signaling, such as the AR antagonist enzalutamide, have been developed (4). For diagnosis and staging of prostate cancer, various imaging modalities are used to determine the extent of the disease. In general, a bone scan is performed to determine whether osseous metastases are present. For detection of lymph node or visceral metastases, PET or CT can be performed. For hormonal treatment to be successful, tumors must express the AR. AR expression can be determined on surgical or biopsy samples, but this would give information about only a small part of a single lesion. Since AR expression can be heterogeneous within and between lesions and can change over time, either spontaneously or as a result of treatment, whole-body information about the AR status of all lesions in a patient would be advantageous. PET imaging with a suitable AR ligand as tracer could provide such information and would enable assessment of receptor occupancy of AR-targeting drugs. Such PET/CT methods for imaging of AR availability could be used not only to depict the extent of the disease but also to identify patients who would benefit from an AR-targeting therapy and to monitor the efficacy of treatment.  $16\beta$ - $^{18}\text{F}$ -fluoro- $5\alpha$ -dihydrotestosterone ( $^{18}\text{F}$ -FDHT) is a radiolabeled analog of  $5\alpha$ -dihydrotestosterone (DHT) and was developed as a PET tracer for AR imaging (5–10).  $^{18}\text{F}$ -FDHT shows high specific binding to the AR but is rapidly metabolized in humans (6). The circulating radiolabeled metabolites bind tightly to plasma proteins, leading to high background activity in blood and low-contrast images. Moreover,  $^{18}\text{F}$ -FDHT metabolites are cleared from the circulation via the kidneys into the urine, a route that can compromise detection of tumors near the prostate. For these reasons, PET tracers with a different excretion route are required for AR imaging.

Unlike  $^{18}\text{F}$ -FDHT, enzalutamide is a pure AR antagonist that possesses an AR affinity similar to that of DHT and is currently used in androgen therapy (11,12). It is known that enzalutamide metabolizes mainly to *N*-desmethylenzalutamide, which has an AR affinity similar to that of the parent compound (13,14). Besides, enzalutamide and *N*-desmethylenzalutamide are excreted primarily via the hepatic route, which would result in low uptake in the kidneys and urine.

In this study, we therefore labeled enzalutamide with  $^{18}\text{F}$  and investigated its potential as a PET tracer for AR imaging (Fig. 1). For this purpose, we performed *in vitro* and *in vivo* studies on a prostate cancer cell line and on castrated and uncastrated mice bearing AR-expressing tumor xenografts. The performance of  $^{18}\text{F}$ -enzalutamide was compared with that of the currently applied tracer,  $^{18}\text{F}$ -FDHT (Fig. 2).

## MATERIALS AND METHODS

FDHT was purchased from PharmaSynth AS (purity  $\geq 95\%$ ), and enzalutamide was provided by Astellas. For radiolabeled compounds, detection on thin-layer chromatography was performed with Cyclone multisensitive phosphor storage screens (Packard). These screens were exposed to the thin-layer chromatography strips for a few seconds and subsequently read using a Cyclone phosphor storage imager (PerkinElmer) and analyzed with OptiQuant software. High-performance liquid chromatography (HPLC) purifications were performed with an Elite LaChrom VWR Hitachi L-2130 pump, using a Waters Symmetry C18 HPLC column, connected to a ultraviolet spectrometer (Elite LaChrom VWR Hitachi L-2400 ultraviolet detector) set at 254 nm and a Bicon frisk-tech radiation detector.

The synthesis and characterization of the nitro precursor (Supplemental Fig. 1), as well as the *in vitro* methods, are presented in the supplemental materials (available at <http://jnm.snmjournals.org>).

PET image reconstruction, data analysis, and *ex vivo* biodistribution were performed as previously described (15). Tracer uptake is expressed as percentage injected dose (%ID)/g.

### Radiosynthesis of $^{18}\text{F}$ -Enzalutamide

Aqueous  $^{18}\text{F}$ -fluoride was produced by irradiation of  $^{18}\text{O}$ -water with a Scanditronix MC-17 cyclotron via the  $^{18}\text{O}(p,n)^{18}\text{F}$  nuclear reaction. The  $^{18}\text{F}$ -fluoride solution was passed through a QMA SepPak Light anion exchange cartridge (Waters) to recover the  $^{18}\text{O}$ -water. The  $^{18}\text{F}$ -fluoride was eluted from the cartridge with 1 mL of  $\text{KHCO}_3$  (1 mg/mL) and collected in a vial with 15 mg of Kryptofix[2.2.2] (Merck). To this solution, 1 mL of acetonitrile was added, and the solvents were evaporated at  $130^\circ\text{C}$ . The  $^{18}\text{F}$ -KF/Kryptofix complex was dried 3 times by the addition of 0.5 mL of acetonitrile followed by evaporation of the solvent.  $^{18}\text{F}$ -enzalutamide was prepared by aromatic nucleophilic fluorination of the corresponding nitro precursor. Thus, the dried  $^{18}\text{F}$ -KF/Kryptofix complex was dissolved in 0.5 mL of *N,N*-dimethylformamide and added to compound 4 (2 mg,  $4.01\ \mu\text{mol}$ ). The reaction mixture was heated at  $150^\circ\text{C}$  for 30 min. After the mixture had cooled, 0.5 mL of water was added. The product was purified by HPLC (eluent, 47% acetonitrile in water; flow, 4 mL/min; retention time, 14 min). The radioactive peak corresponding to the product was collected and diluted with 50 mL of distilled water and passed through

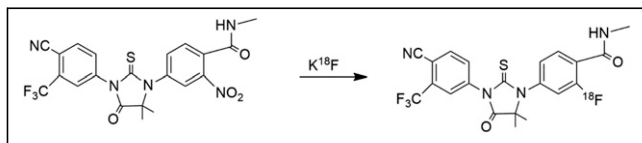


FIGURE 1. Scheme of radiosynthesis of  $^{18}\text{F}$ -enzalutamid.

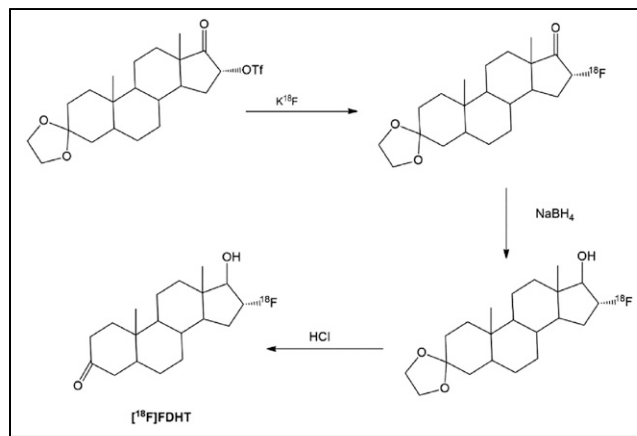


FIGURE 2. Scheme of radiosynthesis of  $^{18}\text{F}$ -FDHT.

an HLB Oasis cartridge (Waters, 30 mg). The product was eluted from the cartridge with 0.8 mL of ethanol and diluted with 4.2 mL of distilled water. Quality control was performed by UPLC, using a BEH Shield RP18 column ( $1.7\ \mu\text{m}$ ,  $3.0 \times 50\ \text{mm}$ ) and 40% aqueous acetonitrile as the mobile phase at a flow of 1 mL/min.

### Radiosynthesis of $^{18}\text{F}$ -FDHT

The fully automated synthesis of  $^{18}\text{F}$ -FDHT was performed as previously described (16).

### Animals

Athymic nude male mice (6–8 wk old) were obtained from Harlan and provided with standard laboratory chow and tap water *ad libitum*. All studies were performed in compliance with the local ethical guidelines for animal experiments. The protocol was approved by the Institutional Animal Care and Use Committee (protocol DEC 6657D). After at least 1 wk of acclimatization, the mice were anesthetized and LNCaP cells (2 million cells in 100  $\mu\text{L}$  of a 1:1 mixture of Matrigel [Corning] and  $\mu\text{L}$  of RPMI with 10% fetal bovine serum) were subcutaneously injected into the neck or shoulder. Approximately 3–4 wk after inoculation, tumor nodules were palpable.

### Surgical Castration

One group of 7 mice was surgically castrated in the third week after tumor inoculation to reduce the levels of circulating androgens. Briefly, the animals were anesthetized using 2% isoflurane and placed on their back. Through a midline scrotal incision, the testes were ligated using Vicryl (Ethicon) and the skin was closed using Vicryl Rapide (Ethicon), after which anesthesia was stopped. Perioperative analgesia was given subcutaneously using Finadyne (Merck), 3 mg/kg. One animal developed a scrotal hematoma.

### Pet Imaging of Xenograft-Bearing Mice

Three to 4 wk after LNCaP cell inoculation, the mice were anesthetized with 2% isoflurane and positioned transversally in the center of the field of view of the small-animal PET camera (Focus 220; Siemens-Concorde).  $^{18}\text{F}$ -enzalutamide ( $14 \pm 7\ \text{MBq}$ ) was mixed with either phosphate-buffered saline (control) or enzalutamide (1 mg/kg) in phosphate-buffered saline and injected via the penile vein.  $^{18}\text{F}$ -FDHT ( $9 \pm 4\ \text{MBq}$ ) was mixed with either phosphate-buffered saline (control) or DHT (1 mg/kg) in phosphate-buffered saline before penile vein injection. Simultaneously with injection of the PET tracer, an emission scan of 60 min was started. After the PET scan was complete, the animals were killed with an overdose of anesthesia, and a 20-min transmission scan with a  $^{57}\text{Co}$  point source was obtained to correct scatter and attenuation of 511-keV photons by tissue. After the

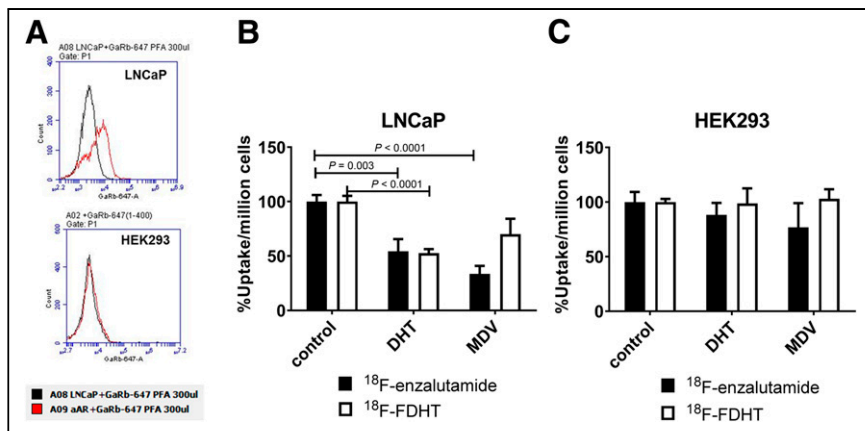


**FIGURE 3.** (A) FACS analysis of AR expression in different cell lines. (A and C) Cell-associated radioactivity of <sup>18</sup>F-enzalutamide and <sup>18</sup>F-FDHT in LNCaP (AR-positive) (B) and HEK293 (AR-negative) (C) cells in absence or presence of unlabeled DHT (1 nM) or MDV (1 nM). Results are expressed as % radioactivity/million cells (mean ± SD).

transmission scan was completed, the animal remained fixed to the bed and the bed was positioned in the CT scanner (Micro-CT II; CTI Siemens). A 15-min CT scan was acquired for anatomic localization of the tumor (exposure time, 1,050 ms; x-ray voltage, 55 kVp; anode current, 500 μA; number of rotation steps, 500; total rotation, 360°).

#### Metabolite Analysis

Acetonitrile, 50 μL, was added to an approximately 25-μL sample of plasma to precipitate the plasma proteins. The samples were centrifuged at 16,000g for 5 min. A 2-μL aliquot of the supernatant was collected and applied on a thin-layer chromatography plate. The thin-layer chromatography plate was eluted with *n*-hexane/ethyl acetate (1:4) ( $R_f$  for <sup>18</sup>F-enzalutamide or <sup>18</sup>F-FDHT, 0.8,  $R_f$  for metabolites, 0.0). After elution, radioactivity on thin-layer chromatography plates was analyzed by phosphor storage imaging. Exposed screens were scanned with a Cyclone phosphor storage system (PerkinElmer), and the percentage of intact <sup>18</sup>F-enzalutamide or <sup>18</sup>F-FDHT as a function of tracer distribution time was calculated by region-of-interest analysis using OptiQuant Software.

#### Statistical Analysis

Statistical analyses were performed with Excel (version 2003; Microsoft) and SigmaPlot (version 10.0; SPSS; Inc.). The values that inhibited 50% of tracer binding were calculated by fitting the data with nonlinear regression using Prism (version 5.0; GraphPad Software). Differences in tracer accumulation between groups were analyzed using the 2-sided unpaired Student *t* test. Significance was reached at a *P* value of less than 0.05. Throughout the article, values are presented as mean ± SD.

## RESULTS

#### Chemistry

The nitro precursor **4** was prepared through a 4-step synthesis with an overall yield of 1.6% (Supplemental Fig. 1) (17,18). The starting material, 2-nitro-4-bromobenzoic acid, was transformed into methyl-2-(3-nitro-4-(methylcarbamoyl)phenylamino)-2-methylpropanoate **3**, which was further reacted with 2-(trifluoromethyl)-4-isothiocyanatobenzonitrile to give the final precursor **4** in 35% yield.

#### Radiochemistry

<sup>18</sup>F-enzalutamide was obtained in 1.4% ± 0.9% radiochemical yield (decay-corrected, based on <sup>18</sup>F-fluoride added to the precursor) within 98 ± 8 min. At the end of synthesis, the apparent

molar activity was 6.2 ± 10.3 GBq/μmol and the radiochemical purity more than 95%. <sup>18</sup>F-FDHT was obtained in a 1.5% ± 0.8% decay-corrected radiochemical yield. The molar activity of <sup>18</sup>F-FDHT was more than 25 GBq/μmol, with a radiochemical purity of more than 95%. <sup>18</sup>F-enzalutamide was stable for at least 60 min in the formulation solution, as no decomposition was observed by UPLC analysis. The distribution coefficients ( $\log D_{7.4}$ ) of <sup>18</sup>F-enzalutamide and <sup>18</sup>F-FDHT were 2.32 ± 0.01 and 2.56 ± 0.01, respectively.

#### In Vitro Binding Affinity

The human embryonic kidney HEK293 cell line is generally considered to be AR-negative, whereas the LNCaP cells are AR-positive. In this study, this belief was confirmed by flow cytometry as depicted in the histograms in Figure 3A, where HEK293 cells did not show any binding of the AR antibody whereas the LNCaP cells stained moderately with the AR antibody.

The in vitro binding affinity of <sup>18</sup>F-enzalutamide and <sup>18</sup>F-FDHT toward AR was evaluated in AR-negative HEK293 and AR-positive LNCaP cells (Figs. 3B and 3C). As expected, the uptake of <sup>18</sup>F-enzalutamide and <sup>18</sup>F-FDHT in HEK293 (AR-negative) could not be saturated with either DHT or enzalutamide. However, <sup>18</sup>F-enzalutamide and <sup>18</sup>F-FDHT uptake in LNCaP (AR-positive) was efficiently blocked with DHT or enzalutamide, suggesting that both tracers selectively bind to AR. This selective binding to AR was further proven with a competitive displacement assay using either <sup>18</sup>F-enzalutamide or <sup>18</sup>F-FDHT and different concentrations of the competitive inhibitors enzalutamide and DHT (Fig. 4). The enzalutamide and DHT concentrations that inhibited 50% of tracer binding in LNCaP cells were 0.22 nM and 1.02 nM, respectively for <sup>18</sup>F-enzalutamide and 1.72 nM and 4.07 nM, respectively, for <sup>18</sup>F-FDHT.

#### In Vivo PET Imaging

<sup>18</sup>F-enzalutamide and <sup>18</sup>F-FDHT PET scans were obtained for LNCaP tumor-bearing athymic nude mice that were injected either with vehicle or with the AR ligand enzalutamide or DHT (Fig. 5). <sup>18</sup>F-enzalutamide PET scans were also obtained for LNCaP tumor-bearing athymic nude mice that were castrated 3 wk after

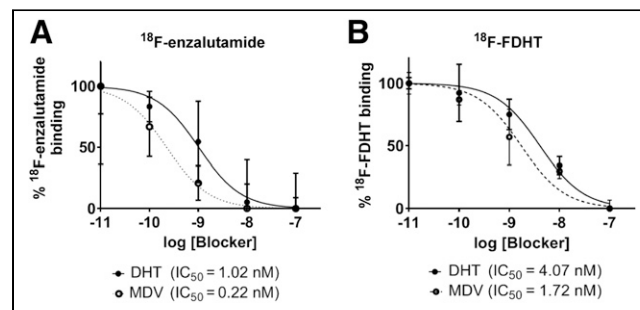


**FIGURE 4.** In vitro competitive AR binding assay of <sup>18</sup>F-enzalutamide (A) and <sup>18</sup>F-FDHT (B) in LNCaP cells, using enzalutamide (MDV) or DHT as competitor.

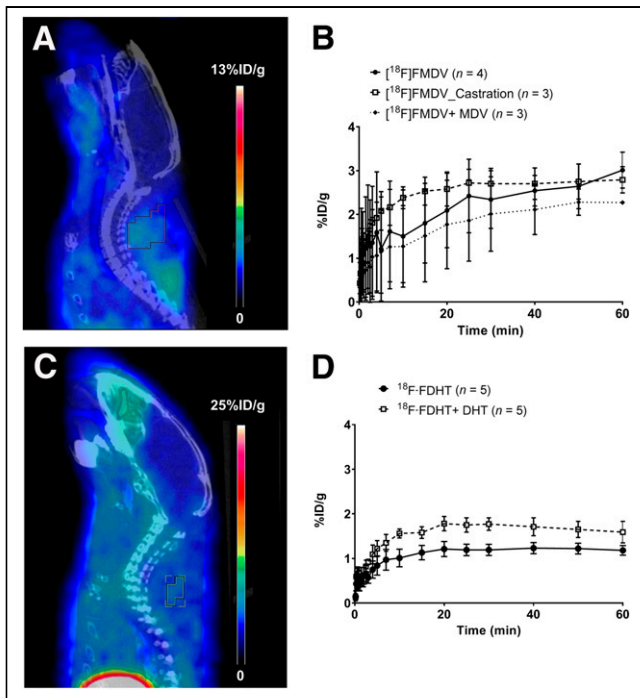


**FIGURE 5.** (A and C) Sagittal small-animal PET/CT fusion images of mouse bearing LNCaP xenograft (delineated) injected with  $^{18}\text{F}$ -enzalutamide ( $14 \pm 7$  MBq) (A) or  $^{18}\text{F}$ -FDHT ( $9 \pm 4$  MBq) (C). (B and D) Time-activity curves of tumor uptake (%ID/g) of  $^{18}\text{F}$ -enzalutamide (B) or  $^{18}\text{F}$ -FDHT (D) in LNCaP xenografts.

tumor inoculation to reduce endogenous testosterone and DHT levels (Supplemental Fig. 2). The time-activity curves of the tumors revealed slow kinetics for both PET tracers. The tracer accumulation in tumors obtained from the last 10 min of the PET scan (50–60 min) were  $3.01 \pm 0.41$  %ID/g (noncastrated) or  $2.95 \pm 0.30$  %ID/g (castrated) for  $^{18}\text{F}$ -enzalutamide and  $1.18 \pm 0.24$  %ID/g (noncastrated) for  $^{18}\text{F}$ -FDHT. Injection of  $^{18}\text{F}$ -enzalutamide together with an excess of enzalutamide resulted in a significant reduction in tumor uptake ( $2.27 \pm 0.03$  %ID/g,  $P < 0.05$ , noncastrated). On the other hand, tumor uptake of  $^{18}\text{F}$ -FDHT was significantly increased when coinjected with DHT ( $1.59 \pm 0.24$  %ID/g,  $P < 0.05$ , noncastrated).

#### Ex Vivo Biodistribution

Ex vivo biodistribution of  $^{18}\text{F}$ -enzalutamide and  $^{18}\text{F}$ -FDHT was evaluated in the animals that had received a PET scan. The results of the biodistribution and blocking experiments are depicted in Table 1. In general,  $^{18}\text{F}$ -enzalutamide exhibited significantly lower uptake in the liver, plasma, and urine ( $P < 0.001$  for all) than did  $^{18}\text{F}$ -FDHT. In contrast, when compared with  $^{18}\text{F}$ -FDHT,  $^{18}\text{F}$ -enzalutamide exhibited significantly higher uptake in some AR-expressing organs, such as the LNCaP xenograft, spleen, and brain, and similar uptake in the small intestine, prostate, and bone (including bone marrow). When  $^{18}\text{F}$ -enzalutamide was coinjected with enzalutamide, uptake in the bone (containing bone marrow,  $P = 0.0001$ ), spleen ( $P = 0.007$ ), small intestine ( $P = 0.03$ ), and LNCaP xenograft ( $P = 0.044$ ) was significantly decreased by 68%, 59%, 56%, and 37%, respectively. As for  $^{18}\text{F}$ -FDHT, when coinjected with DHT the uptake was significantly decreased in the liver ( $P = 0.001$ ), urine ( $P = 0.025$ ), and brown fat ( $P = 0.047$ ). Uptake of  $^{18}\text{F}$ -enzalutamide was significantly higher in the

prostate of castrated mice than in noncastrated animals ( $P = 0.008$ ) but not in any other tissues.

#### Metabolite Analysis

Metabolite analysis revealed that only  $3.1\% \pm 2.1\%$  ( $n = 12$ ) of the total plasma radioactivity consisted of intact  $^{18}\text{F}$ -FDHT at 1 h after injection.  $^{18}\text{F}$ -enzalutamide was more stable in vivo, as  $93\% \pm 14\%$  ( $n = 19$ ) of the plasma activity at 1 h after injection still consisted of the intact tracer.

#### DISCUSSION

This study showed that  $^{18}\text{F}$ -enzalutamide appears to be a suitable PET tracer for imaging of AR expression in androgen-dependent tumors. As such,  $^{18}\text{F}$ -enzalutamide could enable whole-body assessment of the stage of the disease, stratification of patients who could benefit from androgen therapy, and evaluation of treatment efficacy. This study also showed that  $^{18}\text{F}$ -enzalutamide seems to have better properties for imaging of AR expression in prostate cancer than does the currently used PET tracer,  $^{18}\text{F}$ -FDHT.

The optimized radiolabeling of  $^{18}\text{F}$ -enzalutamide consisted of a nucleophilic aromatic substitution reaction of the nitro analog of enzalutamide with  $^{18}\text{F}$ -fluoride, leading to the desired product with yields similar to those for labeling of  $^{18}\text{F}$ -FDHT. Because of a similarity in structure between the nitro precursor and  $^{18}\text{F}$ -enzalutamide, it was not possible to completely separate these 2 compounds by HPLC, leading to an apparent molar activity that was 4 times lower than that of  $^{18}\text{F}$ -FDHT. Because of the structural similarity between the nitro precursor and enzalutamide, it is reasonable to assume that the precursor also might have (some) affinity for the AR. Consequently, the contamination of  $^{18}\text{F}$ -enzalutamide with precursor could have resulted in an underestimation of its binding properties for the AR and, thus, its imaging performance.

To confirm that the  $^{18}\text{F}$ -enzalutamide continues to possess a high affinity toward AR receptors, a competitive radiometric binding assay was performed with both tracers in LNCaP (AR-positive) and Hek293 (AR-negative) cells. Unlabeled enzalutamide and DHT were able to inhibit  $^{18}\text{F}$ -enzalutamide and  $^{18}\text{F}$ -FDHT binding in LNCaP cells, demonstrating that both  $^{18}\text{F}$ -enzalutamide and  $^{18}\text{F}$ -FDHT binding is AR-mediated. Competitive binding assays showed that the binding affinity of  $^{18}\text{F}$ -enzalutamide toward the AR was similar to that of  $^{18}\text{F}$ -FDHT, despite the lower apparent molar affinity of the former tracer. The results of our binding assays agree with data for the unlabeled drug reported in the literature (11).

To evaluate the potential of  $^{18}\text{F}$ -enzalutamide as a PET tracer for in vivo imaging of AR expression, dynamic PET scans and ex vivo biodistribution were performed on LNCaP tumor-bearing athymic nude male mice. First, we evaluated whether castration of male mice would influence uptake in the LNCaP xenografts. Ex vivo biodistribution at 1 h after tracer injection showed a similar distribution of  $^{18}\text{F}$ -enzalutamide in castrated and noncastrated mice. Interestingly, uptake of  $^{18}\text{F}$ -enzalutamide was found to be significantly higher in castrated mice than in noncastrated mice for only the prostate, suggesting that the reduction of low circulating androgen levels increases the sensitivity of the tracer toward AR-expressing organs by reducing the competition with the endogenous ligand. The castration-induced reduction in circulating androgen levels did not result in an increase in tracer uptake in the LNCaP xenograft ( $P = 0.424$ ), possibly because of the relatively high AR expression levels in LNCaP xenografts. In the case of high receptor expression, the effect of the occupancy of the receptor by the endogenous ligand is relatively small. To reduce the

**TABLE 1**  
Biodistribution 1 Hour After Intravenous Injection of  $^{18}\text{F}$ -Enzalutamide or  $^{18}\text{F}$ -FDHT in Castrated and Noncastrated Mice Bearing LNCaP Tumors

Organ	$^{18}\text{F}$ -enzalutamide ( <i>n</i> = 5)*	$^{18}\text{F}$ -enzalutamide + castration ( <i>n</i> = 3) <sup>†</sup>	$^{18}\text{F}$ -enzalutamide + enzalutamide (0.13 $\mu\text{mol/g}$ animal) ( <i>n</i> = 5)*	$^{18}\text{F}$ -FDHT ( <i>n</i> = 5)*	$^{18}\text{F}$ -FDHT + DHT (0.13 $\mu\text{mol/g}$ animal) ( <i>n</i> = 5)*
Bone	3.01 $\pm$ 0.63	2.41 $\pm$ 0.12	0.95 $\pm$ 0.14 <sup>  </sup>	3.04 $\pm$ 0.54	3.18 $\pm$ 1.62
Brain	1.62 $\pm$ 0.71	1.66 $\pm$ 0.32	1.75 $\pm$ 0.43	0.56 $\pm$ 0.07	0.96 $\pm$ 0.54
Brown fat	14.64 $\pm$ 5.60	12.85 $\pm$ 2.44	15.89 $\pm$ 7.81	2.17 $\pm$ 0.70	1.24 $\pm$ 0.35
Heart	4.80 $\pm$ 0.52	5.82 $\pm$ 1.01	4.44 $\pm$ 0.52	2.28 $\pm$ 0.34	2.70 $\pm$ 1.30
Kidney	6.51 $\pm$ 3.01	6.37 $\pm$ 1.00	5.21 $\pm$ 0.52	5.33 $\pm$ 0.84	4.95 $\pm$ 1.86
Liver	14.17 $\pm$ 0.98	12.76 $\pm$ 1.67	8.36 $\pm$ 1.27 <sup>  </sup>	22.76 $\pm$ 3.16	9.91 $\pm$ 4.48 <sup>  </sup>
Lung	3.48 $\pm$ 0.44	5.03 $\pm$ 1.59	3.34 $\pm$ 0.29	2.01 $\pm$ 0.37	2.50 $\pm$ 1.30
Muscle	2.61 $\pm$ 0.51	2.79 $\pm$ 0.16	2.39 $\pm$ 0.83	1.77 $\pm$ 0.38	2.78 $\pm$ 2.47
Plasma	0.89 $\pm$ 0.41	0.61 $\pm$ 0.23	1.40 $\pm$ 1.25	2.58 $\pm$ 0.48	2.24 $\pm$ 1.26
Red blood cells	2.09 $\pm$ 0.64	2.24 $\pm$ 0.27	2.52 $\pm$ 1.48	2.49 $\pm$ 0.54	3.39 $\pm$ 2.51
Spleen	4.66 $\pm$ 1.25	5.26 $\pm$ 1.48	1.89 $\pm$ 0.62 <sup>  </sup>	1.93 $\pm$ 0.30	1.92 $\pm$ 0.87
Prostate	3.37 $\pm$ 1.15	6.15 $\pm$ 0.51 <sup>  </sup>	4.37 $\pm$ 1.41	2.72 $\pm$ 0.80	2.39 $\pm$ 1.40
Urine	0.57 $\pm$ 0.29	0.15 $\pm$ 0.06	0.14 $\pm$ 0.06 <sup>  </sup>	19.84 $\pm$ 6.36	6.53 $\pm$ 7.72
Tumor	5.74 $\pm$ 1.31 <sup>‡</sup>	4.45 $\pm$ 2.65	3.64 $\pm$ 0.26 <sup>§,  </sup>	1.63 $\pm$ 0.22	1.59 $\pm$ 0.82 <sup>‡</sup>

\*One animal showed extravasation during tracer injection.

<sup>†</sup>Three animals showed extravasation during tracer injection.

<sup>‡</sup>One animal did not develop tumor.

<sup>||</sup>*P* < 0.05 (Statistically significant differences between castrated vs. noncastrated and AR blocker vs. vehicle).

<sup>§</sup>Two animals did not develop tumor.

Data are expressed as %ID/g (mean  $\pm$  SD).

complexity of the experiment and animal discomfort, it was decided to demonstrate proof of the principle of specific tracer uptake in LNCaP xenografts by performing the blocking studies with the AR ligands enzalutamide and DHT in noncastrated mice.

Although both tracers had similar lipophilicities, they showed somewhat different distribution patterns.  $^{18}\text{F}$ -FDHT showed significantly higher accumulation in the liver, plasma, and urine than  $^{18}\text{F}$ -enzalutamide did. On the other hand,  $^{18}\text{F}$ -enzalutamide had significantly higher uptake in brown fat than  $^{18}\text{F}$ -FDHT did. One reason for these differences could be the difference between in vivo stabilities. The metabolite analysis in plasma indicated that  $^{18}\text{F}$ -enzalutamide remained mostly intact during the time of the experiment (1 h), whereas  $^{18}\text{F}$ -FDHT was almost completely metabolized into less lipophilic compounds, which are likely excreted into the urine.

The time-activity curves of the tumors revealed slow kinetics for both PET tracers. However, the  $^{18}\text{F}$ -enzalutamide accumulation in LNCaP tumors was about 3 times higher than that of  $^{18}\text{F}$ -FDHT. In addition, the animals that were coinjected with an excess of unlabeled enzalutamide showed significantly decreased tumor uptake of  $^{18}\text{F}$ -enzalutamide, when compared with the ones that were coinjected with the vehicle. This result was confirmed by the results of the ex vivo biodistribution, suggesting that tumor uptake of  $^{18}\text{F}$ -enzalutamide is receptor-mediated. Such AR-mediated tumor uptake could not be demonstrated for  $^{18}\text{F}$ -FDHT. Surprisingly, PET revealed that uptake of  $^{18}\text{F}$ -FDHT in the LNCaP xenograft was not reduced but, rather, was increased by coinjection with an excess of DHT. However, such an increase was not confirmed by the results of the ex vivo biodistribution study,

which did not reveal any difference in  $^{18}\text{F}$ -FDHT uptake between DHT and vehicle-treated animals. The discrepancy between the PET and ex vivo biodistribution results might be due to difficulty in localizing tumors in PET images or to a partial-volume effect caused by the small size of the tumors (<0.1 cm<sup>3</sup>), potentially causing spillover of background activity.

This proof-of-concept study had several limitations that need to be addressed. First, several mice did not develop LNCaP tumors; thus, a relatively low number of animals remained for statistical analysis. In addition, the scans and ex vivo studies with  $^{18}\text{F}$ -enzalutamide perhaps should have been done later, since at 60 min tracer uptake is still increasing. Another limitation was the relatively low apparent molar activity of  $^{18}\text{F}$ -enzalutamide due to contamination with the precursor. Despite extensive optimization of the HPLC purification method, we could not completely remove the precursor from the product. Thus, another synthesis route should be investigated using a precursor that is easy to separate from the product. A possible solution could be to replace the nitro precursor by the corresponding trimethylammonium precursor. Nonetheless, even with a low apparent molar activity,  $^{18}\text{F}$ -enzalutamide appeared to be a suitable PET tracer for imaging ARs in tumors.

## CONCLUSION

$^{18}\text{F}$ -enzalutamide can readily be radiolabeled with  $^{18}\text{F}$ , with yields similar to those of  $^{18}\text{F}$ -FDHT, although the apparent molar activity is relatively low.  $^{18}\text{F}$ -enzalutamide is highly stable in vivo, and that fact that it shows less accumulation in the liver, plasma, and urine is advantageous when evaluating local metastasis near

the prostate. These promising preclinical results warrant further preclinical and clinical evaluation.

## DISCLOSURE

This study was funded by the PCMM project of the Center for Translational Molecular Medicine (CTMM). No other potential conflict of interest relevant to this article was reported.

## ACKNOWLEDGMENTS

We thank Jürgen W.A. Sijbesma for helping with the in vivo study and Astellas Pharma Europe for providing the enzalutamide.

## KEY POINTS

**QUESTION:** Is  $^{18}\text{F}$ -enzalutamide more suitable than  $^{18}\text{F}$ -FDHT as a PET tracer to access AR expression in vivo?

**PERTINENT FINDINGS:**  $^{18}\text{F}$ -enzalutamide shows higher tumor uptake, better metabolic stability, and lower plasma uptake than  $^{18}\text{F}$ -FDHT in vivo and thus seems to have more favorable properties for imaging of AR with PET, producing images with higher contrast.

**IMPLICATIONS FOR PATIENT CARE:** The fact that  $^{18}\text{F}$ -enzalutamide has the same structure as the AR signaling inhibitor may enable a better understanding of AR signaling inhibitor-targeted drug development. In addition, by having more favorable properties as a PET tracer,  $^{18}\text{F}$ -enzalutamide potentially may be used to more effectively select patients who would respond to such therapies and to monitor their effectiveness.

## REFERENCES

1. Fitzmaurice C, Dicker D, Pain A, et al. The global burden of cancer 2013. *JAMA Oncol.* 2015;1:505–527.
2. Shafi AA, Yen AE, Weigel NL. Androgen receptors in hormone-dependent and castration-resistant prostate cancer. *Pharmacol Ther.* 2013;140:223–238.
3. Nader R, El Amm J, Aragon-Ching JB. Role of chemotherapy in prostate cancer. *Asian J Androl.* 2018;20:221–229.
4. Scott LJ. Enzalutamide: a review in castration-resistant prostate cancer. *Drugs.* 2018;78:1913–1924.
5. Larson SM, Morris M, Gunther I, et al. Tumor localization of  $^{16}\beta$ - $^{18}\text{F}$ -fluoro-5 $\alpha$ -dihydrotestosterone versus  $^{18}\text{F}$ -FDG in patients with progressive, metastatic prostate cancer. *J Nucl Med.* 2004;45:366–373.
6. Beattie BJ, Smith-Jones PM, Jhanwar YS, et al. Pharmacokinetic assessment of the uptake of  $^{16}\beta$ - $^{18}\text{F}$ -fluoro-5-dihydrotestosterone (FDHT) in prostate tumors as measured by PET. *J Nucl Med.* 2010;51:183–192.
7. Fox JJ, Gavane SC, Blanc-Autran E, et al. Positron emission tomography/computed tomography-based assessments of androgen receptor expression and glycolytic activity as a prognostic biomarker for metastatic castration-resistant prostate cancer. *JAMA Oncol.* 2018;4:217–224.
8. Scher HI, Beer TM, Higano CS, et al. Antitumour activity of MDV3100 in castration-resistant prostate cancer: a phase 1–2 study. *Lancet.* 2010;375:1437–1446.
9. Vargas HA, Kramer GM, Scott AM, et al. Reproducibility and repeatability of semiquantitative  $^{18}\text{F}$ -fluorodihydrotestosterone uptake metrics in castration-resistant prostate cancer metastases: a prospective multicenter study. *J Nucl Med.* 2018;59:1516–1523.
10. Glaudemans AWJM, de Vries EFJ, Luurtsema G, et al. Detection of intra-abdominal testicles with  $^{16}\beta$ - $^{18}\text{F}$ -fluoro-5 $\alpha$ -dihydrotestosterone positron emission tomography/computed tomography in a pubertal boy. *J Pediatr.* 2015;166:774–4.e1.
11. Tran C, Ouk S, Clegg NJ, et al. Development of a second-generation antiandrogen for treatment of advanced prostate cancer. *Science.* 2009;324:787–790.
12. Gauthier S, Martel C, Labrie F. Steroid derivatives as pure antagonists of the androgen receptor. *J Steroid Biochem Mol Biol.* 2012;132:93–104.
13. Highlights of prescribing information: Xtandi<sup>®</sup> (enzalutamide) capsules for oral use. U.S. Food and Drug Administration website. [https://www.accessdata.fda.gov/drugsatfda\\_docs/label/2012/2034151bl.pdf](https://www.accessdata.fda.gov/drugsatfda_docs/label/2012/2034151bl.pdf). Revised August 2012. Accessed March 9, 2021.
14. Kim T-H, Jeong J-W, Song J-H, et al. Pharmacokinetics of enzalutamide, an anti-prostate cancer drug, in rats. *Arch Pharm Res.* 2015;38:2076–2082.
15. Antunes IF, van Waarde A, Dierckx RA, de Vries EG, Hospers GA, de Vries EF. Synthesis and evaluation of the estrogen receptor  $\beta$ -selective radioligand 2- $^{18}\text{F}$ -fluoro-6-(6-hydroxynaphthalen-2-yl)pyridin-3-ol: comparison with  $^{16}\alpha$ - $^{18}\text{F}$ -fluoro-17 $\beta$ -estradiol. *J Nucl Med.* 2017;58:554–559.
16. Khayum MA, Doorduyn J, Antunes IF, et al. In vivo imaging of brain androgen receptors in rats: a [ $^{18}\text{F}$ ]FDHT PET study. *Nucl Med Biol.* 2015;42:561–569.
17. Jung ME, Ouk S, Yoo D, et al. Structure–activity relationship for thiohydantoin androgen receptor antagonists for castration-resistant prostate cancer (CRPC). *J Med Chem.* 2010;53:2779–2796.
18. Jain RP, Angelaud R, Thompson A, Lamberson C, Greenfield S, inventors; Medivation Prostate Therapeutics, Inc., assignee. Processes for the synthesis of diarylthiohydantoin compounds. European Patent EP2538785B1, 2081. September 1, 2011.